

The Structure of High Pressure $\text{Ca}(\text{OD})_2$ II from Powder Neutron Diffraction: Relationship to the ZrO_2 and EuI_2 Structures

Kurt Leinenweber, Dan E. Partin, Udo Schuelke, and Michael O’Keeffe

Department of Chemistry, Arizona State University, Tempe, Arizona 85287

and

Robert B. Von Dreele

MLNSCE, Los Alamos National Laboratory, Los Alamos, New Mexico 87545

Received December 2, 1996; in revised form April 15, 1997; accepted April 21, 1997

The “unquenchable” high pressure form of $\text{Ca}(\text{OH})_2$ [$\text{Ca}(\text{OH})_2$ II] has been synthesized at 9 GPa and 400°C and recovered to ambient pressure at cryogenic temperatures. The structure was determined from powder neutron diffraction data using the Rietveld technique. The symmetry is monoclinic $P2_1/c$ with $a = 5.3979(4)$ Å, $b = 6.0931(4)$ Å, $c = 5.9852(4)$ Å, $\beta = 103.581(6)^\circ$, $Z = 4$ at 1 atm and 11 K. $R_{\text{wp}} = 2.8\%$, $R_p = 1.9\%$, reduced $\chi^2 = 6.6$ for 117 variables. The calcium and oxygen substructure is intermediate between that in $\alpha\text{-PbO}_2$ and that in fluorite; it was previously described as isostructural with baddeleyite (ZrO_2), but it is more accurately described as isostructural with EuI_2 . This structure is distinguished by the presence of a 3^d anion net parallel to (100). Only one of the two kinds of D atoms in the structure shows appreciable hydrogen bonding to O, with a second neighbor D ... O distance of 1.91 Å, and an O–D ... O angle of 153.2°; the other D atom has 3 second-neighbor oxygens near 2.6 Å away. © 1997 Academic Press

INTRODUCTION

The high pressure form of $\text{Ca}(\text{OH})_2$, named $\text{Ca}(\text{OH})_2$ II by Kunz *et al.* (1), is synthesized by heating the ambient-pressure portlandite phase to 200°C or higher at pressures above 7 GPa. This material exhibits a powder diffraction pattern markedly different from that of portlandite. So far, characterization of this phase has been limited to *in situ* high pressure work, because during decompression at room temperature the $\text{Ca}(\text{OH})_2$ II reverts to portlandite. Kunz *et al.* indexed the powder X-ray pattern and located the Ca and O atoms in the structure by using a diamond-anvil cell combined with monochromatic synchrotron radiation and an imaging plate. The structure is monoclinic, $P2_1/c$, with $Z = 4$ and all atoms in general positions. Kunz *et al.* de-

scribed the CaO_2 part of the structure as isostructural with the low-temperature form of ZrO_2 (baddeleyite).

A further understanding of the high pressure $\text{Ca}(\text{OH})_2$ structure would add considerably to the known systematics of simple hydroxides, since this represents a new example among only a small number of structures known so far. There is also considerable interest in the correlation between vibrational parameters, hydrogen bonding, and structure in these and related materials (2). The present study was designed to obtain a full refinement of the high pressure $\text{Ca}(\text{OH})_2$ structure, including location of the hydrogen atoms, using powder neutron diffraction. This is presently difficult to do with *in situ* high pressure techniques for neutron diffraction (3) because of small sample size, stress, and the necessity of heating the sample under pressure to obtain the high pressure form—experimental problems which are compounded by the low symmetry of the compound (five atoms in general positions). The present study used a sample that was recovered at low temperature in an apparatus which pumps liquid nitrogen past a multianvil high pressure synthesis assembly during decompression (4).

EXPERIMENTAL

A deuterated strating sample of portlandite, $\text{Ca}(\text{OD})_2$, was prepared as follows: CaCO_3 (Baker) was decomposed to CaO in a covered Pt crucible at 960°C in air, the crucible was then removed from the oven, plunged immediately into liquid nitrogen, and transferred to a desiccator to avoid icing. The highly reactive CaO was subsequently converted to $\text{Ca}(\text{OD})_2$ by placing into boiling D_2O (Aldrich) for 5 min in a covered flask.

The $\text{Ca}(\text{OD})_2$ was dried and checked by Raman spectroscopy to ensure that a significant amount of H was not present. The sample showed a strong OD stretching peak,

and the OH stretching peak was absent, verifying a sample close to $\text{Ca}(\text{OD})_2$ in composition. X-ray diffraction was used to verify that $\text{Ca}(\text{CO})_3$ and other potential impurities were not present in detectable quantities. Samples (60 mg) were then pressed and wrapped in platinum foil and treated at 9 GPa and 400°C for 1 h in a multiple anvil device in the Materials Research Group laboratory at Arizona State University. While still maintaining high pressure, the temperature was quenched to 298 K in a few seconds by shutting off the power. Following this, liquid nitrogen was introduced into the sample area, and the sample was decompressed cold (near 77 K) and recovered to a cryogenic storage Dewar flask. Individual samples of about 60 mg of the “frozen-in” high-pressure form of $\text{Ca}(\text{OD})_2$ could be made in this way. A test (4) using a low-temperature stage and Raman spectroscopy indicated that the reversion to portlandite begins near 220 K, so care was taken to keep the sample temperature well below this by transferring the samples rapidly.

The cryogenic decompression process was repeated three times in order to obtain 180 mg of high-pressure $\text{Ca}(\text{OD})_2$. The platinum foil used to wrap the samples for the high pressure runs was left on the samples to be used as a low temperature d -spacing standard. For the neutron diffraction experiment using the high-intensity neutron powder diffractometer (HIPD) at MLNSCE, Los Alamos National Laboratories, the samples were transferred under helium to a vanadium sample can partially immersed in liquid nitrogen; the can was closed with an Ir wire seal and placed into an already cold Displex. The sample chamber was evacuated (this also served to remove ice from the outside of the sample can) and the sample was further cooled to 11 K. A data set was collected over 24 h using six detector banks located at ± 151 , ± 90 , and $\pm 40^\circ$.

The diffraction pattern showed $\text{Ca}(\text{OD})_2$ II + Pt, with no sign of portlandite, carbonate, or ice peaks, indicating that the sample preparation and transfer techniques were suitable. Rietveld refinement of data from all six banks was performed using the program GSAS (5), using a minimum d -spacing of 0.371 Å. The relationship between TOF and d -spacing was calibrated for each bank using $a = 3.9155$ Å for Pt at 11 K (6). The starting model for Ca and O in $\text{Ca}(\text{OD})_2$ was from Kunz *et al.*, and the D starting locations were obtained from a Fourier difference map.

Refinement with unconstrained thermal parameters led to various negative values, depending on the model used. It was found that constraining the thermal motions for Ca, O(1), and O(2) to be equal led to all positive thermal parameters, with large thermal motions of the D atoms; because this was the most general model for which all thermal parameters are physical, it is presented as the primary structural model here. An identical (within 1 SD) structure was obtained by letting all thermal parameters vary independently and using anisotropic thermal parameters for D,

but a principal axis of the thermal ellipsoid on D(2) had a small negative value. The final refinement of 34,675 data points fitted with 117 variables led to $R_{\text{wp}} = 2.8\%$, $R_p = 1.9\%$, reduced $\chi^2 = 6.6$. Typical histograms showing the fit to the data are shown in Fig. 1.

RESULTS

The structural parameters for the final model of $\text{Ca}(\text{OH})_2$ II are listed in Table 1. The table also shows the lattice parameters and the Ca and O positions of Kunz *et al.* (1) for comparison. The lattice parameters of the two studies differ significantly because of the difference in pressure and temperature between the two data sets, but the internal parameters for Ca and O are close. This indicates that both data sets are taken on the same phase, although under different conditions. The monoclinic angle in the present study is larger by a few degrees, indicating a significant dependence of the angle on pressure. The density of the recovered material is about 12% greater than that of portlandite, which is very similar to the result obtained in the high pressure study (1). A projection of the 11 K, 0.1 MPa structure along the b -axis is shown in Fig. 2 (bottom right).

Selected bond lengths for $\text{Ca}(\text{OH})_2$ II are given in Table 2 together with bond valence sums (7) for the atoms. The structure solution, including deuterium positions, looks reasonable, since all the valence sums are close to the expected atomic valences. O(1) and D(1) both appear slightly underbonded; this is related to the refined O(1)–D(1) bond length being slightly longer than the expected 0.96 Å.

D(2) is bonded to O(2) but also has a near O(1) neighbor 1.91 Å away, suggesting normal D(2)...O(1) hydrogen bonding. The angle associated with this bonding is O–D...O = 153.2°. On the other hand, D(1) [bonded to O(1)] has three O(2) neighbors at a distance of 2.57–2.60 Å away, distances normally considered too long for hydrogen

TABLE 1
Structural Parameters for $\text{Ca}(\text{OD})_2$ II Obtained in the Present Study at 11 K and 0.1 MPa Compared with Data [in Brackets] at 298 K and 9.5 GPa (1)

Atom	x	y	z	$100 \times U_{\text{iso}}$
Ca	0.3057(5) [0.3254]	0.0722(4) [0.0624]	0.1880(4) [0.2011]	0.11(2) ^a
O(1)	0.0688(4) [0.104]	0.3727(4) [0.395]	0.2765(4) [0.271]	0.11(2) ^a
O(2)	0.4150(4) [0.375]	0.7628(4) [0.764]	0.4960(4) [0.505]	0.11(2) ^a
D(1)	0.1472(5)	0.4946(5)	0.2052(4)	2.24(7)
D(2)	0.2334(6)	0.7762(4)	0.4378(4)	2.41(7)

Note. $P2_1/c$, $a = 5.3979(4)$ [4.887] Å, $b = 6.0931(4)$ [5.384] Å, $c = 5.9852(4)$ [5.587] Å, $\beta = 103.581(6)^\circ$, [99.74°], $V = 191.34(1)$ [157.0].

^a Thermal motions of Ca, O(1), and O(2) constrained to be equal.

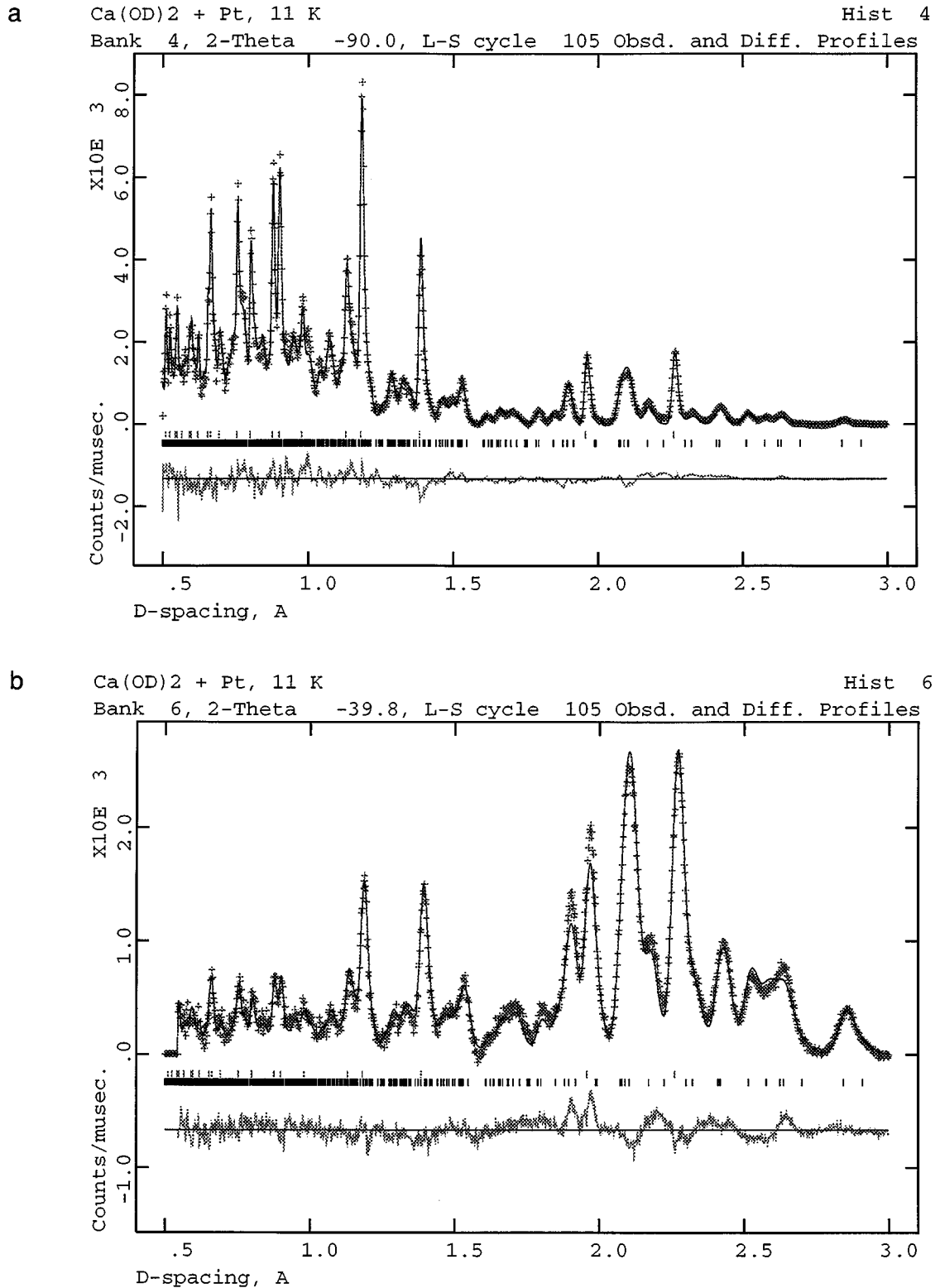


FIG. 1. TOF neutron diffraction profile fit to (a) data from a 90° bank and (b) data from a 40° bank, from 0.5 to 30\AA . The background has been subtracted from both plots. The data are shown as “+”, and the solid line is the calculated profile. Tick marks below the pattern show the positions of Pt diffraction lines (upper row of tick marks) and $\text{Ca}(\text{OD})_2$ II diffraction lines (lower row). The difference curve (observed – calculated) is shown at the bottom of each plot.

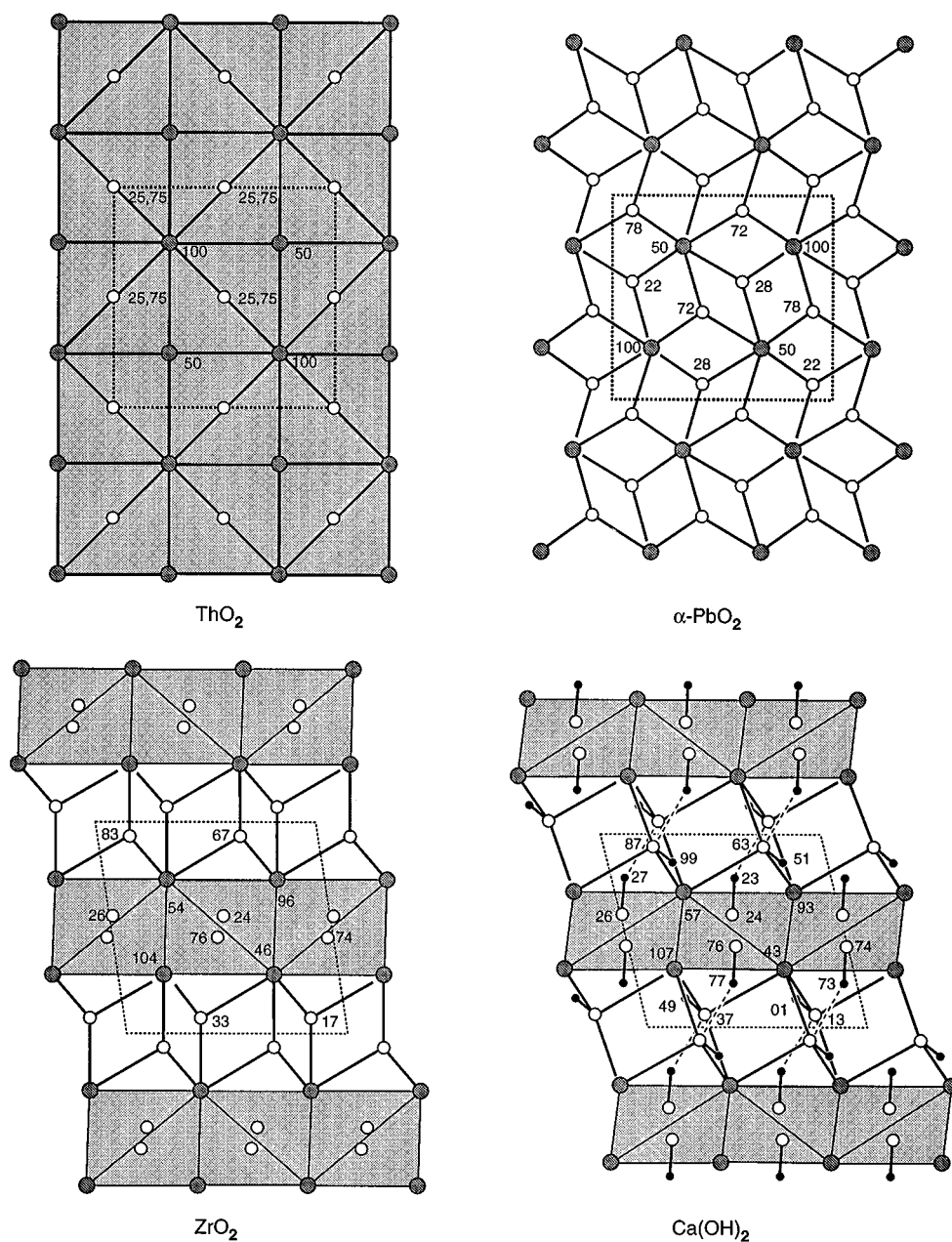


FIG. 2. Comparison of the structures of ThO_2 , $\alpha\text{-PbO}_2$, ZrO_2 and Ca(OH)_2 . The largest circles are metal atoms, and the smallest are hydrogen atoms and layers of O-centered tetrahedra of metal atoms are shaded. For $\alpha\text{-PbO}_2$ the projection is on (100) of $Pbcn$ with \mathbf{b} horizontal; numbers are elevations in multiples of $a/100$. For ZrO_2 and Ca(OH)_2 the projection is on (010) of $P12_1/c1$ with \mathbf{c} horizontal; numbers are elevations in multiples of $b/100$.

bonding (8). The shortest D...D distances are $D(1)\dots D(2) = 2.19$ and 2.25 \AA .

Calcium is in 7-coordination to oxygen in the structure with three Ca–O(1) distances ranging from 2.36 to 2.52 \AA and four Ca–O(2) distances ranging from 2.35 to 2.61 \AA . The wide range of Ca–O distances is rather surprising. In the absence of hydrogen bonding, the Brown equal valence rule (9) leads one to expected valences of $\nu = 1/3$ for Ca–O(1)

and $\nu = 1/4$ for Ca–O(2); the corresponding expected (7) bond lengths are $d[\text{Ca–O}(1)] = 2.37 \text{ \AA}$ and $d[\text{Ca–O}(2)] = 2.48 \text{ \AA}$. However the bond valence sum at Ca ($V = 1.99$) is very close to the expected $V = 2$, so we can be fairly confident of the accuracy of the structure determination. In ZrO_2 (10) the corresponding range of distances is $d[\text{Zr–O}(1)] = 2.05\text{--}2.16 \text{ \AA}$ and $d[\text{Zr–O}(2)] = 2.15\text{--}2.29 \text{ \AA}$ — a significantly smaller spread.

TABLE 2
Bond Lengths, Bond Valences, and Valence Sums
in Ca(OD)₂ II

Bond	Length	Valence	Sum	Bond	Length	Valence	Sum
Ca–O(1)	2.3634(1)	0.342		O(1)–Ca	2.3634(1)	0.342	
Ca–O(1)	2.4106(1)	0.302		O(1)–Ca	2.4106(1)	0.302	
Ca–O(1)	2.5168(2)	0.226		O(1)–Ca	2.5168(2)	0.226	
Ca–O(2)	2.3495(2)	0.355		O(1)–D(1)	0.9992(1)	0.876	
Ca–O(2)	2.3694(1)	0.337		O(1)–D(1)	2.5957(1)	0.012	
Ca–O(2)	2.4807(1)	0.249		O(1)–D(2)	1.9156(2)	0.074	1.820
Ca–O(2)	2.6059(1)	0.178	1.990	O(2)–Ca	2.3495(2)	0.355	
D(1)–O(1)	0.9992(1)	0.876		O(2)–Ca	2.3694(1)	0.337	
D(1)–O(1)	2.5957(1)	0.012		O(2)–Ca	2.4807(1)	0.249	
D(1)–O(2)	2.5707(2)	0.012		O(2)–Ca	2.6059(1)	0.178	
D(1)–O(2)	2.5867(1)	0.012	0.876	O(2)–D(2)	0.9638(1)	0.963	
D(2)–O(2)	0.9638(1)	0.964		O(2)–D(1)	2.5707(2)	0.012	
D(2)–O(1)	1.9156(2)	0.074	1.037	O(2)–D(1)	2.5867(1)	0.012	2.084

DISCUSSION

Figure 2 compares the structures of monoclinic zirconia (baddeleyite) (10), ThO₂ (used as an oxide example of the fluorite structure) and α -PbO₂ (11) with the structure of Ca(OH)₂II (now generalized from Ca(OD)₂ for the purpose

of discussion). Notice in the ZrO₂ and Ca(OH)₂ structures that one O atom is four-coordinated to a metal atom in approximately tetrahedral coordination in layers in the same way as O in ThO₂ (F in CaF₂); the other O atom is three-coordinated and the layers of these atoms are very similar to layers in the structure of α -PbO₂. The structures of baddeleyite and Ca(OH)₂ (both with seven-coordinated cations) can therefore be described as intermediate between the α -PbO₂ structure (with six-coordinated cations) and the fluorite structure (with eight-coordinated cations). In all four of these structures the cation arrangement is approximately cubic close packed (exactly in TbO₂) so that to derive one from another the main atomic displacements are those of the anions.

It should be apparent from Fig. 2 that the structures of baddeleyite and Ca(OH)₂ differ in detail. The substructure of the Ca and O atoms (i.e., the structure of Ca(OH)₂ if the H are ignored) is in fact closer to that of EuI₂ (12) and NdSBr (13). This structure was first described in (12), where it was recognized as distinct from the ZrO₂ structure because of differences in the shape of the sevenfold cation polyhedra. The difference may also be readily seen by examining layers of the structures parallel to (100) as illustrated in Fig. 3. In both Ca(OH)₂ and ZrO₂, the four-coordinated

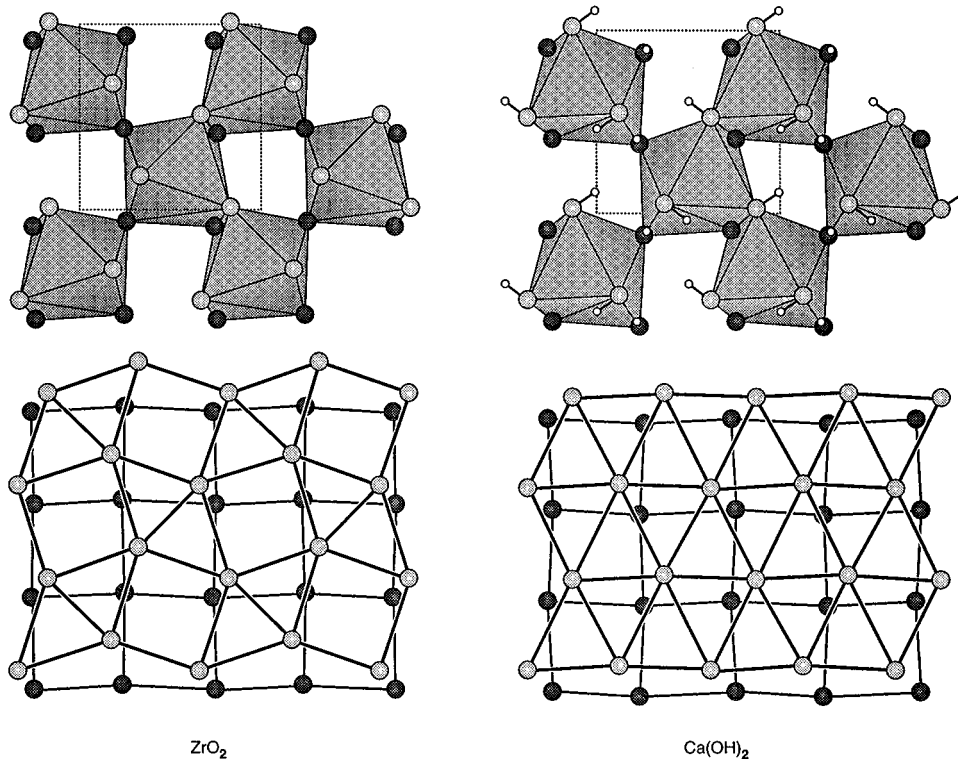


FIG. 3. (Top) A (100) layer of Ca(OH)₂ and ZrO₂ showing a layer of MO₇ cation-centered polyhedra. H atoms in Ca(OH)₂ are shown as small circles; the larger circles are O atoms with O(2) darker shaded. The O(2)–D(2) bonds are approximately normal to the plane of projection and half the D(2) atoms are occluded by the circles representing O(2). (Bottom) The same layers with the anion nets emphasized.

O atoms are on 4^4 nets (as in fluorite). The primary difference between the two structures lies in the arrangement of the three-coordinated atoms (which are shown more lightly shaded in the figure). In ZrO_2 the three-coordinated O atoms are on $3^2.4.3.4$ nets. In $Ca(OH)_2$ the three-coordinated atoms form 3^6 nets; this is in fact the arrangement in EuI_2 . The two kinds of layer can also be easily distinguished by examining the coordinates of anion X(1) (in the labelling of this paper). As shown in Table 3 the y and z coordinates of these atoms are both approximately equal to 0.36 for $3^2.4.3.4$ nets, and the coordinates in ZrO_2 approach this value. For 3^6 nets $y \approx 0.36$ and $z \approx 0.25$; as may be seen in the table the parameters in both EuI_2 and $Ca(OH)_2$ are close to these values. Another difference is that the 4^4 layer is more puckered, as shown by the larger deviation of the x parameter for anion X(2) from the theoretical value of 0.5 for a flat net. HfO_2 (14) forms an intermediate case, containing a $3^2.4.3.4$ net which is somewhat distorted towards a 3^6 net.

Although the difference between the ZrO_2 and EuI_2 structures is subtle, and requires a structural refinement in order to be demonstrated, it is nonetheless a useful distinction. Physically, the two structures may represent different phases, and careful studies might reveal isosymmetric phase transitions between them for some compounds. The occurrence of an intermediate net in HfO_2 also points toward the alternate possibility of a continuous change between the two structures. In either case, it is proposed that the EuI_2 structure is the higher pressure form, since the presence of the close-packed 3^6 net combined with the stronger puckering of the 4^4 net leads to a more contracted structure. This is supported by the fact that ZrO_2 itself has a pressure-induced phase transition to an EuI_2 -related structure: the high pressure orthorhombic form of ZrO_2 (15) is composed of a stacking of two EuI_2 -type layers along a , in which one EuI_2 (100) layer alternates with its mirror image.

Recent work on hydroxide structures under pressure has focused on the effect of pressure on hydrogen bonding (16) and whether as a general rule hydrogen bonding "increases"

with pressure. If second neighbor oxygen distances are used as a structural measure of hydrogen bonding (2), then it is apparent in the present case that hydrogen bonding is more pronounced in $Ca(OH)_2$ II than in portlandite. In portlandite, the three second neighbor oxygens are at a distance of 2.66 Å, meaning that hydrogen bonding must be very weak (8). In $Ca(OH)_2$ II, O(2) has three second neighbors, at 2.57, 2.59 and 2.60 Å, and is similar overall to the environment in portlandite, at least in terms of oxygen neighbors. O(1), on the other hand, has one oxygen second neighbor at 1.92 Å, indicative of hydrogen bonding. Therefore, across the phase transition there is little change in the bonding of half of the hydrogen atoms and a significant increase in the bonding of the other half. This increase in bonding may be correlated with the large change in density of the material. Interestingly, the two hydrogen environments and degree of hydrogen bonding are similar to those in the ambient-pressure phase of $Sr(OH)_2$ (18). Like $Ca(OH)_2$ II, the $Sr(OH)_2$ structure has the cations in seven-coordination with oxygen, although the linkage of the polyhedra is different.

As a final note, we find it interesting that the hydroxide structure is that of an iodide (EuI_2) rather than an oxide (ZrO_2). Despite the fact that F and OH can often substitute for one another as in complex structures such as that of the apatites, it seems that simple hydroxides often have iodide (or other heavier halide) rather than fluoride structures. Indeed the low pressure structure (with six-coordinated cations) of $Ca(OH)_2$ and brucite, $Mg(OH)_2$, is the same as that of CaI_2 and MgI_2 (CdI_2 type) rather than a structure such as one of those favored by oxides and fluorides (e.g., rutile for MgF_2) and lighter halides such as $CaCl_2$ or $MgCl_2$ (17). Recently attention has also been drawn (18) to the similarity between the structures of $Sr(OH)_2$ and SrI_2 . A possible explanation is that the highly polarizable iodide ion will adopt a position of lower symmetry (19) and thus better mimic the polar OH group.

ACKNOWLEDGMENTS

The authors acknowledge the support of the NSF Materials Research Group for Synthesis of High Pressure Materials (DMR-91 21570) and Grants EAR-9628678 (K.L.) and DMR 94 24445 (M.O.K.). This work has benefitted from the use of facilities at the Manual Lujan, Jr. Neutron Scattering Center, a national user facility funded as such by the DOE/Office of Basic Energy Sciences.

REFERENCES

1. M. Kunz, K. Leinenweber, J. B. Parise, T.-C. Wu, W. A. Bassett, K. Brister, D. J. Weidner, M. T. Vaughan, and Y. Wang, *High Pressure Res.* **14**, 311 (1996).
2. H. D. Lutz, *Struct. Bonding* **82**, 85 (1995).
3. J. M. Besson and R. J. Nelmes, *Physica B* **213**, 31 (1995).
4. K. Leinenweber, U. Schuelke, and S. Ekbundit, "High Pressure-Temperature Research: Properties of Earth and Planetary Materials." Proceedings of the 1996 US-Japan Seminar, in press.

TABLE 3

Anion Parameters for High Pressure $Ca(OH)_2$ II (Present Study) Compared with Theoretical Values for Planar Anion Nets and Measured Values for EuI_2 (7) and ZrO_2 (8)

	$Ca(OH)_2$ II	EuI_2	ZrO_2	$3^6/4^4$ nets	$3^2.4.3.4/4^4$ nets
X(1) x	0.069	0.099	0.070	0.000	0.000
X(1) y	0.373	0.391	0.336	0.360	0.361
X(1) z	0.276	0.284	0.341	0.250	0.361
X(2) x	0.415	0.424	0.442	0.500	0.500
X(2) y	0.763	0.770	0.755	0.750	0.750
X(2) z	0.496	0.495	0.479	0.500	0.500

5. A. C. Larson and R. B. Von Dreele, "GSAS: General Structure Analysis System". Los Alamos National Laboratory, Los Alamos, NM, 1994.
6. R. K. Kirby, *Int. J. Thermophys.* **12**, 679 (1991).
7. N. E. Brese and M. O'Keeffe, *Acta Crystallogr. B* **47**, 192 (1991).
8. C. B. Aakeröy and K. R. Seddon, *Chem. Soc. Rev.* **22**, 397 (1994).
9. I. D. Brown, *Acta Crystallogr. B* **48**, 553 (1992).
10. D. K. Smith and H. W. Newkirk, *Acta Crystallogr.* **18**, 983 (1965).
11. R. J. Hill, *Mater. Res. Bull.* **17**, 769 (1982).
12. H. Barnighausen and N. Schultz, *Acta Crystallogr. B* **25**, (1969).
13. N. Savigny, C. Adolphe, A. Zalkin, and D. H. Templeton, *Acta Crystallogr.* **29**, 1532 (1973).
14. R. Ruh and P. W. R. Corfield, *J. Am. Crystallograph. Soc.* **53**, 126 (1970).
15. Y. Kudoh, H. Takeda, and H. Arashi, *Phys. Chem. Miner.* **13**, 233 (1986).
16. J. B. Parise, K. Leinenweber, D. J. Weidner, K. Tan, and R. B. Von Dreele, *Am. Miner.* **79**, 193 (1994).
17. A. F. Wells, "Structural Inorganic Chemistry," 5th ed. Clarendon Press, Oxford, UK, 1984.
18. D. E. Partin and M. O'Keeffe, *J. Solid State Chem.* **119**, 157 (1995).
19. W. R. Busing, *Trans. Am. Crystallogr. Soc.* **6**, 57 (1970)